Journal of Nanomedicine & Biotherapeutic Discovery

Eshita et al., J Nanomed Biotherapeut Discov 2012, 2:5
DOI: 10.4172/2155-983X.1000109

Research Article Open Access

Supramolecular Targeting of B16F10 Melanoma Cells With Nanoparticles Consisting of a DEAE-Dextran-MMA Copolymer-Paclitaxel Complex *In vivo and In vitro*

Yuki Eshita[1]*, Rui-Cheng Ji[2], Masayasu Onishi[3], Lucky Ronald Runtuwene[1], Kaori Noguchi[1], Takashi Kobayashi[1], Masaaki Mizuno[4], Jun Yoshida[5], Naoji Kubota[6] and Yasuhiko Onishi[3]*

[1]*Department of Infectious Disease Control, Oita University, 1-1 Idaigaoka, Hasama-machi, Yufu, Oita 879-5593, Japan*
[2]*Department of Human Anatomy, Oita University, 1-1 Idaigaoka, Hasama-machi, Yufu, Oita 879-5593, Japan*
[3]*Ryujyu Science Corporation, 39-4 Kosora-cho, Seto, Aichi 489-0842, Japan*
[4]*The Center for Advanced Medicine and Clinical Research, Nagoya University Hospital, 65 Tsurumai-cho, Showaku, Nagoya, Aichi 466-8560, Japan*
[5]*Chubu Rosai Hospital, Japan Labor Health and Welfare Organization, 1-10-6 Komei, Minato-ku, Nagoya, Aichi 455-8530, Japan*
[6]*Department of Chemistry, Oita University, 1-1 Idaigaoka, Hasama-machi, Yufu, Oita 879-5593, Japan*

Abstract

A DEAE-dextran-MMA copolymer (DDMC)-paclitaxel (PTX) complex was obtained by using PTX as the guest and DDMC as the host. The resulting nanoparticles of the DDMC/PTX complex were 50-300 nm in diameter and are confirmed to be useful as an anti-cancer drug forming a stable polymeric micelle in water. The drug resistance of B16F10 melanoma cells to paclitaxel was observed using survival curve analysis. On the other hand, there is no drug resistance of melanoma cells to the DDMC/PTX complex. The DDMC/PTX complex showed superior anti-cancer activity to paclitaxel alone *in vitro*. The cell death rate was determined using Michaelis-Menten kinetics, as the DDMC/PTX complex promoted allosteric supramolecular reaction to tubulin. The DDMC/PTX complex showed a very superior anti-cancer activity to paclitaxel alone *in vivo* in mouse skin. The median survival time (MST) of the saline, PTX, DDMC/PTX4 (particle size 50 nm) and DDMC/PTX5 (particle size 290 nm) groups were 120 hours (T/C, 1.0), 176 hours (T/C, 1.46), 328 hours (T/C, 2.73), and 280 hours (T/C, 2.33), respectively. It will be deduced different chemo-effect on melanoma cells between PTX group and DDMC/PTX-treated mice group from this result.

From our results, the DDMC/PTX complex was not extensively degraded in cells, and achieved good efficacy as an intact supramolecular anti-cancer agent. The DDMC/PTX complex showed high reactivity and specificity of anti-melanoma cells, depending on its supramolecular facilities. The DDMC/PTX complex represents the efficacy as supramolecular intact such as artificial enzymes having substrate-selective. These supramolecular facilities to melanoma cells will be very helpful to overcome cancer diseases.

Keywords: Supramolecule; DEAE-dextran-MMA copolymer; Paclitaxel; Melanoma cells

Introduction

The resistance of cancer cells to chemotherapeutic drugs (MDR) is a major problem to successful cancer chemotherapy. The resist ability of cancer cells to survive exposure to various anticancer drugs presents the biggest obstacle to successful cancer chemotherapy [1].

Drug delivery systems (DDS) based on polymers have been used as important carriers for targeted drug delivery because of their enhanced permeability and retention (EPR) effect [2] and their avoidance of the reticuloendothelial system (RES) [3-4]. Recent studies have provided new insights into the intracellular distribution and efficacy of polymer-based DDS. For example, triple-labeled confocal microscopy of living cells revealed the localization of micelles (i.e., the drug-carrying polymer complex) in several cytoplasmic organelles, including the mitochondria, but not in the nucleus [5-6]. Moreover, the cellular distribution of the micelle could be altered, and could increase the amount of drug delivered to the cells. These micelles may thus be worth exploring for their potential to selectively deliver drugs to specified sub-cellular targets [7]. Supramolecule is the compounds of the intermolecular bond, covering the structures and functions of molecular self-assembly, folding, molecular recognition and host-guest chemistry formed by association of two or more chemical species [8].

Materials and Methods

DDMC-paclitaxel complexation

The DDMC–paclitaxel complex was obtained by adding paclitaxel as a guest to 5 ml of 2% DDMC. Paclitaxel (PTX) (a) 2.3 mg, (b) 7.7 mg, (c) 14.2 mg were clathrated in 10 ml of 19.2% aqueous solution of dextran-MMA copolymer grafted rate 100%, the resulted complex by DDMC/PTX (a), (b), and(c) were obtained . To investigate the physical properties of these products, thermal analysis and infrared analysis were carried out.

***Corresponding authors:** Yuki Eshita, Department of Infectious Disease Control, Oita University, 1-1 Idaigaoka, Hasama-machi, Yufu, Oita 879-5593, Japan, E-mail: yeshita@oita-u.ac.jp

Yasuhiko Onishi, Ryujyu Science Corporation, 39-4 Kosora-cho, Seto, Aichi 489-0842, Japan, E-mail: VYX00545@nifty.com

Received December 12, 2012; **Accepted** December 26, 2012; **Published** January 08, 2013

Citation: Eshita Y, Ji RC, Onishi M, Runtuwene LR, Noguchi K, et al. (2012) Supramolecular Targeting of B16F10 Melanoma Cells With Nanoparticles Consisting of a DEAE-Dextran-MMA Copolymer-Paclitaxel Complex *In vivo* and *In vitro*. J Nanomed Biotherapeut Discov 2: 109. doi:10.4172/2155-983X.1000109

Characterization of the DDMC-paclitaxel complex

IR spectra were recorded on a Horiba FT-720 spectrophotometer by the KBr pellet method. The resolution was 2 cm^{-1} and 100 single-averaged scan was taken. The scan rate was 2.5 cm^{-1}. Differential scanning calorimetry (DSC) was run on a Seiko Instrument DSC 6100 under N_2 atmosphere at the flow rate of 20 cm^3/min. Each powder sample (1.5 ± 0.1 mg) was introduced into an aluminum sample pan and previously cooled down to -10°C. After keeping at the temperature for 30 min, the heating scan was done up to 300°C at the heating rate of 10°C/min. The temperature was calibrated with pure indium. Particle size distribution and the ζ-potential of the DDMC-paclitaxel complex were measured using dynamic light scattering and particle electrophoretic mobility (SZ-100 nanoparticle series instrument; HORIBA, Ltd.). Scanning electron microscopy of freeze-dried DDMC-paclitaxel complex was done using a HITACHI S-4800 (Hitachi). Absorbance of the DDMC-paclitaxel complex in solution was measured at a wavelength of 227 nm and in light path of 10 mm using a NanoDrop200c (Thermo Fisher Scientific Inc.).

MTT (WST8) assay

Cell survival was determined using MTT assays with water-soluble tetrazolium salts, a series of water-soluble dyes suitable for MTT assays. The optical density of each well was measured at 450 nm and cell survival was calculated using the following formula:

Cell survival (%)=$[(A_s-A_b)/(A_c-A_b)]\times100$

Where A_s=absorbance of the sample, A_c=absorbance of the control well (no cells) and A_b=absorbance of the blank well.

In vivo test

Female mice (C57BL/6N Sea; 6weeks old and weighing 14-21 g) were purchased from Kyudo Co., Ltd. (Saga, Japan). Experiments using mice were approved by and carried out according to the guidelines of the Animal Ethics Committee of Oita University (N009001, Oita, Japan). To evaluate the acute toxicity of the conjugates, mice were administered PTX and DDMC/ PTX copolymer by a single i.p. injection.

To evaluate the anti-tumor effect of PTX or DDMC/PTX, tumor-bearing mice were prepared by inoculating Melanoma Cells B16F10 cells subcutaneously onto the back of C57BL mice (2.0×10^6 cells/mouse). 12 days after inoculation, PTX and DDMC/PTX complex were administrated by i.p. injection three times on days 12, 14, and 16. Tumor size was measured with a digital vernier caliper (DT-100, Niigata seiki Co., LTD.) and the volume was calculated using V (mm^3)=$(a\times b^2)/2$, where a is the longer, and b is the shorter diameter. The survival rate was also monitored at 2 days intervals.

Results

DDMC-paclitaxel complex

A complex consisting of DDMC and paclitaxel (DDMC-paclitaxel) was obtained by using an anti-tumor alkaloid paclitaxel (PTX) as the guest and DDMC as the host. The particle size distribution and ζ-potential of the DDMC/PTX complex were measured by dynamic light scattering and particle electrophoretic mobility. Furthermore, scanning electron microscopy (SEM) (Figure 1A) was used to determine the size and shape of the freeze-dried DDMC/PTX complex(DDMC/PTX5), which revealed the complex formed uniform cubic particles with a diameter of 200-300 nm on dynamic light scattering. Particle

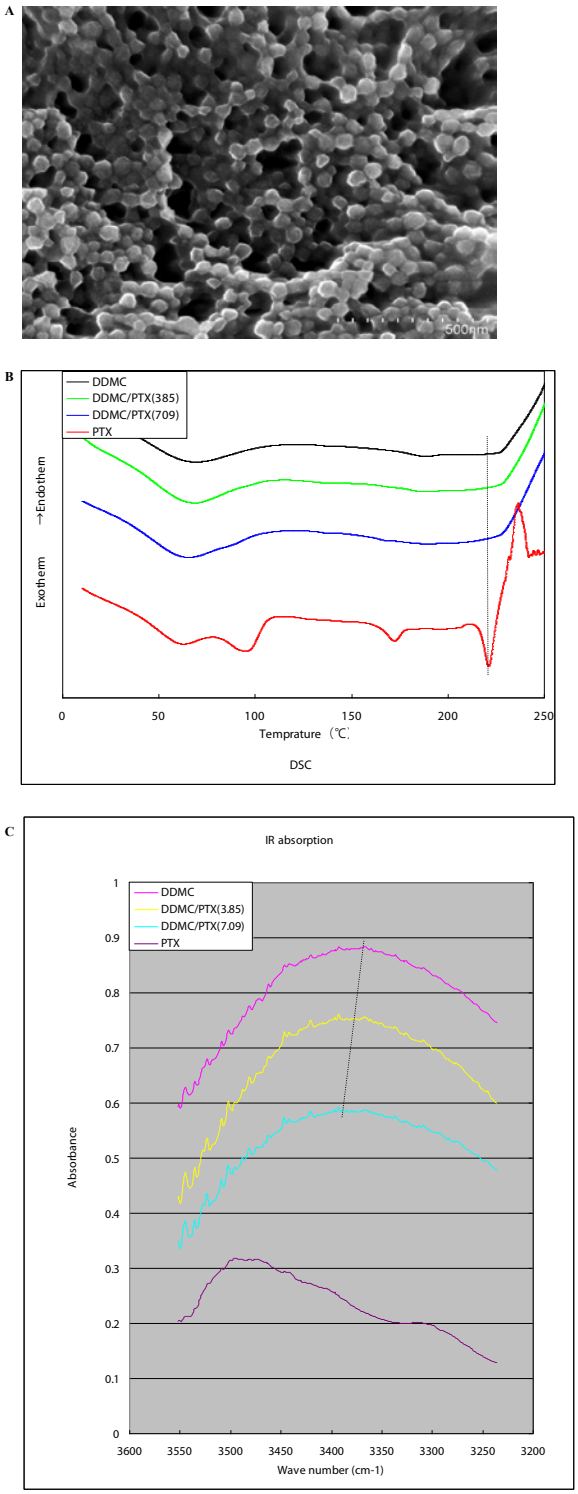

Figure 1: Characteristics of the DDMC-paclitaxel complex. A) Scanning electron microscopic image (HITACHI S-4800) of the freeze-dried DDMC-paclitaxel complex taken at an accelerating voltage of 5 kV. B) Differential scanning calorimetry (DSC) with DDMC-paclitaxel complex and paclitaxel: 1) DDMC, 2) DDMC/PTX complex (DDMC 9.6 mg/PTX 0.385 mg), 3) DDMC/PTX complex (DDMC 9.6 mg/PTX 0.709 mg), and 4) PTX. C) IR absorption spectra of the DDMC-paclitaxel complex and paclitaxel: 1) DDMC, 2) DDMC/PTX complex (DDMC 9.6 mg/PTX 0.385 mg), 3) DDMC/PTX complex (DDMC 9.6 mg/PTX 0.709 mg), and 4) PTX.

size determined by SEM (Figure 1A) was 300-500 nm. The ζ-potential of the particles, outside of the electric double layer, was +36 mV, which contributes to stabilize the dispersion of the DDMC/PTX complex. Considering that the particle size of DDMC may be approximately 25 nm, it seems that the DDMC/PTX complex forms clusters to make stable polymeric micelles.

Absorbance of DDMC/PTX complex in solution was measured at a wavelength of 227 nm (light path, 10 mm) to decide absorbance coefficient (ε) of 62.4×10^4 $M^{-1}cm^{-1}$ [9]. This is much larger than that of paclitaxel alone, which was 3.27×10^4 $M^{-1}cm^{-1}$ in acetone/H_2O (50:1), 2.8×10^4 $M^{-1}cm^{-1}$ in CH_3CN:H_2O (4:1) and 2.6×10^4 $M^{-1}cm^{-1}$ in MeOH:H_2O (1:1). This increase in absorbance may be due to promoting π-electron resonance, which forms a line dependent on the supramolecular π stack structure of paclitaxel self-integrated into DDMC [10]. These properties may also explain why the DDMC/PTX complex showed high reactivity and specificity for its target substrate in melanoma cells which are known broadly as the most lethal cancer cell having many MDR genes.

To investigate the physical properties of these products, thermal analysis and infrared analysis were carried out using PTX (b) 7.7 mg and (c) 14.2 mg of PTX clathrated in 10 ml of 19.2% aqueous solution of dextran-MMA copolymer grafted rate 100%.

Figure 1B shows the Differential Scanning Calorimetry (DSC) curves of PTX and the complex by DDMC/PTX (c), where the ordinate scale was normalized with PTX content. As shown in figure 1B, PTX revealed an exothermic peak (4) following three distinctive exothermic peaks (1-3).

1. Elimination of non-structural water which is adsorbed on a sample (94.9°C).
2. Dehydration of the paclitaxel dihydrate (171.8°C)
3. The melting point of paclitaxel (220.8°C) ΔHm=20.6 mJ/mg
4. Decomposition temperature (236°C)

On the other hand, in case of the complex DDMC/PTX (b, c), the endothermic peak corresponding to the melting point of 220.8°C did not appear in (b) and (c). From this, it is considered that PTX has been the non-crystalline at the inclusion in the complex by DDMC/PTX.

Figure 1C shows infrared absorption spectrum of DDMC (graft rate: 102%)(a), DDMC/PTX complexes (b, c) and PTX (d) at the wave number of 3200-3700 cm^{-1}.

The large and broader absorption due to the stretching vibration of the hydrogen bonded N-H, O-H, and NH-O is observed near 3400 cm^{-1} for the DDMC/PTX complexes and DDMC, whereas the absorption peak in the vicinity of 3500 cm^{-1} for PTX of the starting material. Moreover, the absorption of N-H and O-H for the DDMC/PTX complexes has shifted rather high energy side than DDMC, the starting material.

This means that the association with the hydrogen bond itself is weakened, which then reassembled supramolecule hydrophobic complexes of them, DDMC by the binding of PTX decreases the entropy than the state to which it is not bound. It is considered that the decrease is expected to be stable against a supramolecular stress. These things when considered attributed to the conformational change happening in each of supramolecular stress.

However, it has become larger when a change of shift to the high-energy side, of the absorption of the complex by DDMC/PTX.

The hydrophobic bond will be folded into three-dimensional structure by the driving force.

Figure 1C shows more broad absorption by C-H stretching vibration near 3000 cm^{-1} in the complex by DDMC/PTX compared with DDMC.

Figure 1C also shows the presence of a large hydrophobic binding in the complex by DDMC/PTX from the above.

Survival analysis for melanoma cells *in vitro*

The results of survival analysis *in vitro* by a direct MTT assay (WST8) showed the efficacy of paclitaxel on melanoma cells from a positive correlation between cell number and absorbance (i.e., optical density). Melanoma cells are well known to show resistance to paclitaxel, as indicated in the survival convex curve shown in figure 2A with asymptote of P(A) and P(B).

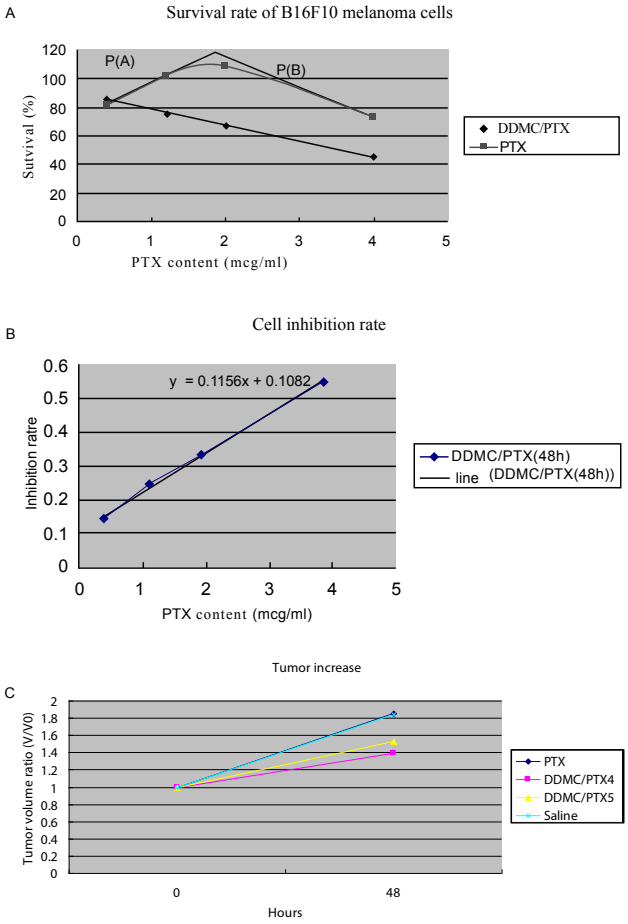

Figure 2: Survival of B16F10 melanoma cells treated with paclitaxel or the DDMC-paclitaxel complex.

A) Survival of B16F10 melanoma cells treated with paclitaxel or the DDMC-paclitaxel complex for 48 hours determined using the MTT (WST8) method.

B) B Tubulin polymerization and cell death (Cd) rates can be expressed by enzymatic kinetic parameters. Relationship between Cd and paclitaxel concentration.

C) The mean tumor volumes increase rate in the PTX, saline, DDMC/PTX4 (size: 50 nm) and DDMC/PTX5(size: 290 nm) groups.

The survival curves, which have a peak-out to PTX concentrations, indicate that MDR gene expression should be taken into account for the concentration-dependent survival at low PTX concentrations (event A) and is negatively associated with survival at higher concentrations of paclitaxel (event B). In this way, the probability of survival is expressed as the product of the probability of P(A) survival positively and P(B) survival negatively, represented as A∩B, where the probability of survival is the product of the probability P(A) from survival positively depending on low PTX concentrations and the probability P(B) of survival negatively depending on high PTX concentrations. Thus, the probability A∩B is the phenomenon that events A and B occur in event (A, B). When events A and B are independent of each other, the probability P (A∩B) is represented by the following formula.

$$P(A \cap B)=P(A)\times P(B)$$

Where: P(A∩B)=probability of event A and B; P(A)=the probability of event A and P(B)=the probability of event B. Using this equation, the convex curve is used to assume that P(A) and P(B) are asymptotic.

For explaining this event A showing MDR, for example, Dr. Miyano of the University of Tokyo has conducted extensive research into the resistance of melanoma cells to PTX. The survival of melanoma cells resistant to paclitaxel has been extensively analyzed using DNA microarrays and dynamic Bayesian analyses. In such studies, gene expression was measured for 24 hours after treatment, which showed that gene clustering over time in melanoma cells. These findings obtained from dynamic Bayesian analysis in combination with non-linear regression were confirmed using data from DNA microarrays [11].

In this experiment, it can be explained using factor analysis to examine the effects of survival and gene expression of melanoma cells on low PTX concentrations. However, we can consider that PTX is unlikely not to participate in stabilization of tubulin (i.e., tubulin polymerization), even at low paclitaxel concentrations. At high concentrations, the enhanced tubulin polymerization will be progress, unable to inhibit the responses to paclitaxel. Therefore, the survival of melanoma cells should be dependent on the threshold dose of PTX concentrations. This phenomenon means that the effect of a medicine does not become remarkable, if, in other words, PTX does not overcome the potential MDR barrier conditionally from resistance gene of taxol at low concentration.

Although the height of a potential barrier is called activation energy, that is, a reaction object molecule must get over in order to exceed the barrier of big energy in this process, and it will turn out that high-concentration of PTX is required as shown in figure 5.

By contrast, the responses of melanoma cells to the DDMC/PTX complex are much more specific without MDR (event A). Of note, the increase in number of melanoma cells were markedly inhibited at low concentrations of the DDMC/PTX complex, having a linear negative correlation between PTX concentration $[E]_0$ and survival rate, following Michaelis-Menten kinetics. This means there are no these resistances of melanoma cells to DDMC/PTX complex, namely MDR.

Michaelis-Menten kinetics

To put it in other words, the relationship between the cell death (Cd) rate (Cd/dt) and tubulin polymerization (P) rate (dp/dt) will assume the following equation, as modified from Cheng and Prusoff [12]:

$$Cd/dt=a\ dp/dt+C_1 \quad (1)$$

Where, a is a constant and C_1 is a device constant corresponding to a>0, C_1>0. The rate of tubulin polymerization V=dp/dt can also be expressed using a Michaelis-Menten Eq. derived its S-shaped curve, as follows

$$v = \frac{\kappa cat[E]_0[S]_0^n}{[S]_0^n + Km} \quad (2)$$

Where Km=Michaelis constant, $[S]_0$= initial tubulin concentration and n=Hill coefficient. In this case, because n>1, mutual interactions between numerous points occur, which fit an S-shaped curve. The stability of the enzyme-substrate complex is shown as 1/km, and larger for DDMC/ PTX complex than for PTX alone, corresponding to $[S]_0^n$ >>Km. The equation

$$v = \kappa cat[E]_0 \quad (3)$$

can be substituted with the expression from (1), as follows:

$$Cd / dt = a\kappa cat[E]_0 + C_1 \quad (4)$$

and integrated into:

$$Cd = a\kappa cat[E]_0 t + C_1 t \quad (5)$$

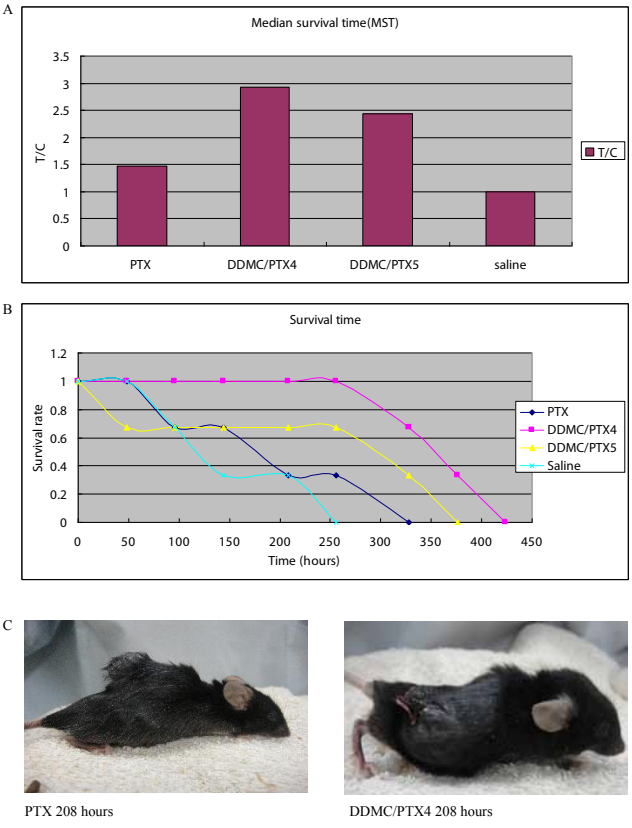

Figure 3: *In vivo* analysis for melanoma cells is investigated by C57BL/6 female mouse. A) The median survival time (50%, MST) of the PTX, saline, DDMC/PTX4 (size: 50 nm) and DDMC/PTX5 (size: 290 nm) groups.

B) The relationships between survival rate and time (hours) with the PTX, saline, DDMC/PTX4 (size: 50 nm) and DDMC/PTX5 (size: 290 nm) groups.

C) Two mice of PTX group and DDMC/PTX4 group after 208 hours from I.P.

From this, the rate of tubulin polymerization V can be expressed using enzymatic parameters for Cd. In these equations, $[E]_0$=initial paclitaxel concentration as an enzyme.

In figure 2B, incubation with MTT for 48 hours yielded the following equation:

$$Cd=0.1062[E]_0 + 0.0481 \quad (6)$$

Thus, 0.0481 represents the constants for $[E]_0$ at 48 hours, respectively.

From Eq. 5, the plots of C_1t with time t are extrapolated to 0 at t=0. Accordingly, when C_1t=0.1082 at 24 hours and 0.0481 at 48 hours are plotted, it can be almost extrapolated to 0 at time t=0 from our previous report [13]. This confirms correctly the assumption in Eq. 5 that the relationship between $[E]_0$ for PTX and the probability of Cd forms a straight line. From these results, the DDMC/PTX complex may promote tubulin polymerization enzymatically that can be expressed using Michaelis-Menten kinetics added the Hill coefficient [14]. These phenomena also show the supramolecular properties of the DDMC/PTX complex.

Survival analysis for melanoma cells *in vivo*

In vivo analysis for melanoma cells is investigated by C57BL/6 female mouse. Anti-tumor effects and survival rates were investigated in tumor-bearing mice.

To evaluate the anti-tumor effect of DMMC/PTX complex, tumor-bearing mice were prepared by inoculating B16F10 melanoma cells S.C. onto the back of C57BL/6 female mouse (2.0×10^6 cells/mouse). At average 1885 mm^3 of tumor volume, 12 days after inoculation, paclitaxel (PTX), DMMC/PTX4 (particle size 50 nm), DMMC/PTX5 (particle size 290 nm), and saline were administrated by I.P. injection three times (at a dose of 10 mg PXL/kg, on days 12, 14, and 16). Tumor size was measured with a digital vernier caliper and the volume was calculated using the relation V (mm^3)=($a\times b^2$)/2 where a is the longer, and b is the shorter diameter. The survival periods also were monitored at 2 days intervals.

Anti-tumor effects and survival of tumor-bearing mice for supramolecular DDMC/PTX complex were very superior to PTX alone.

The tumor growth inhibitory activities were evaluated using B16F10 in xeno-graft tumor-bearing C57BL/6 mice. As shown in figure 2C, the tumors rapidly grew in size when the mice were treated with saline and PTX. This means for PTX, there is no effective facility of anti-tumor growth. But DDMC/PTX complex has more controlled to inhibit cancer growth than saline and PTX, and showed remarkable cancer growth inhibition as down to 46% after the 48 hours. The mean tumor volumes increase rate after the 48 hours in the PTX, saline, DDMC/PTX4 and DDMC/PTX5 groups were 1.85, 1.84, 1.39 and 1.53, respectively. Same times, at 24 hours after I.P., the tumors of DDMC/PTX4 and DDMC/PTX5 groups change from a cycle form to an ellipse form. But one of PTX and saline groups were still a cycle form. This tumor strain means that DDMC/PTX complex inhibits cancer growth by promoting α,β tubulin polymerization to give a strong stress to cytoskeleton or its anti-angiogenic reaction.

The effects of the drugs on the survival of tumor-bearing mice were also evaluated, and the survival data are summarized in figure 3A. The median survival times (50%, MST) of the saline, PTX, DDMC/PTX4 and DDMC/PTX5 groups were 120 hours (T/C, 1.0), 176 hours (T/C, 1.46), 352 hours (T/C, 2.93), and 292 hours (T/C, 2.43), respectively.

Figure 3B shows the relation between survival rate and time (hours) with the PTX, saline, DDMC/PTX4 (size: 50 nm) and DDMC/PTX5 (size: 290 nm) groups.

The mice treated with saline and PTX showed more short survival rate.

In contrast, it was far longer survival of 280-328 hours in DMC/PTX4 and DDMC/PTX5-treated mice.

As shown in figure3B, very interestingly, the mice treated with saline and PTX showed more gradually the decrease in survival from early time of the experiment.

On the other hand, it appears no change with time for longer survival of 250 hours in DDMC/PTX4 and DDMC/PTX5-treated mice.

It will be deduced there different chemo-effect on melanoma cells between PTX group and DDMC/PTX -treated mice group from this result. Efficacy of DDMC/PTX4-treated mice group on inhibiting melanoma tumor was also superior to DDMC/PTX5 group owing to its small particle size 50nm (EPR effect). *In vivo* drug efficacy of DDMC/PTX on cancer cells should depend on its EPR effect, avoidance of the RES, and supramolecular enzymatic function.

Figure 3C shows two mice of PTX group and DDMC/PTX4 group after 208 hours from I.P.

A mouse of DDMC/PTX4 group was almost curing after small dermatophagia owing to its anti-angiogenesis.

It will be the hemorrhagic necrotic symptom of tumor by the release of "TNF-α" cytokine.

DDMC/PTX complex will better react to melanoma cells at the point of metastasis.

Discussion

Allosterical enzymatic reactions

The results from figures 2 and 3 have only recognized MDR of melanoma cells to PTX.

There exists no definite MDR of melanoma cells to DDMC/PTX complex. The results will indicate that these enzymatic reactions allosterically promote tubulin polymerization in cells for DDMC/PTX complex. In DDMC/PTX complex, hydrophobic interactions between the polymer and substrate, with PTX located in so-called the hydrophobic pocket, allow PTX to selectively react with tubulin as indicated in figure 4A.

This effect is not apparent with PTX alone, and is less susceptible to interference from other signals.

Allosterical enzymatic reactions are effective to the conformational changes that occur in the α-β tubulin dimer in the presence of the drug [15]. The results also provide evidence that the DDMC/PTX complex causes a supramolecular reaction involving allosteric promotion, as in Eq. 2. The Hill coefficient included in Eq. 2 supports the likelihood of allosteric cooperation as it represents the strength of cooperative molecular joints. These may depend on the supramolecular facility of clathrate compounds like the PTX as guest is complexed with DDMC as the host. Therefore, the DDMC/PTX complex shows marked substrate specificity as artificial enzymes. This substrate specificity of the DDMC/PTX complex promotes enzymatically a reaction between PTX and tubulin and avoids potential interference from changes in

gene expression that may affect the survival response to PTX, even at low concentrations.

The DDMC/PTX complex is not degraded in the cell, and its efficacy may be enhanced by remaining in supramolecular form.

Thermodynamic consideration of supramolecular allosteric binding

PTX cannot overcome the potential MDR barrier conditionally from resistance gene of taxol at low concentration.

This phenomenon is easily understood by transition state theory for enzymatic reactions. Supramolecular allosteric binding is a phenomenon that increases the reactivity between the active site and other substrate-binding site. Binding of the molecule to the allosteric binding site on one subunit enhances the affinity of the other binding sites by inducing structural conformation changes.

Electrostatic and hydrophobic interactions between the DDMC/PTX complex and its substrate, the α, β-tubulin dimer, orientate β-tubulin with the hydrophobic pocket of the DDMC/PTX complex, which promotes to polymerize the α, β-tubulin dimer through the activity sight of PTX following Michaelis-Menten kinetics. The stability of the enzyme (DDMC/PTX)-substrate (α,β-tubulin dimer) complex (Michaelis complex) can be represented as 1/Km, although probably very large, it causes dynamic instability in the tubulin dimers to stop the Treadmill of tubulin Protomers. This α, β-tubulin dimer and DDMC/PTX complex also contain Mg^{2+} and GTP on the leading edge, which may also be involved in tubulin polymerization, as follows:

$$nTaTb+GTP+Mg^{2+}+DDMC\text{-}paclitaxel \rightarrow Complex \rightarrow (TaTb)n+GDP+Mg^{2+}+DDMC\text{-}paclitaxel \quad (7)$$

where T_aT_b is the α, β-tubulin dimer.

In the case of enzyme-substrate interactions with DDMC/PTX complex to melanoma cells B16F10, the allosteric properties from supramolecule must yield entropy decreases (entropy trap) depending on the selective reaction with tubulin and the strain of substrate under its stress from molecular structure form allosterically as indicated in figure 4A.

At the same time, an enthalpy decreases produce depending on adhesion of substrate by DDMC/PTX complex.

The catalytic power of enzymes which efficiently form transition states has been proposed to involve an equilibrium between the Michaelis complex and a stabilized transition state.

Gibbs free energy in the transition state is considered as follows:

$$\Delta G^{\ddagger}=\Delta H^{\ddagger}-T\Delta S^{\ddagger} \quad (8)$$

Where, $\Delta G^{\ddagger}$ means free energy of activation, $\Delta S^{\ddagger}$ means entropy of activation, and $\Delta H^{\ddagger}$ also means enthalpy of activation.

Figure 5 shows a potential energy curve and activation energy Ea.

Where, $Ea \fallingdotseq \Delta H^{\ddagger}$

With PTX, many signals from gene expression in melanoma cells propose a huge $\Delta G^{\ddagger}$ owing to large $\Delta S^{\ddagger}$ and large $\Delta H^{\ddagger}$ as in figure 5.

As $R \propto e\Delta H^{\ddagger}/RT$ with apoptosis for melanoma cell(R), melanoma cell can overcome the efficacy of PTX in a low concentration.

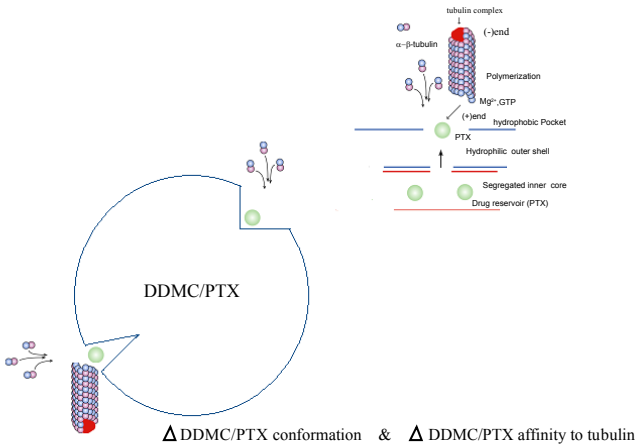

Figure 4: Schematic representation of α,β-tubulin dimer polymerization showing the allosteric relationship between the DDMC-paclitaxel complex and α,β-tubulin. Simplified structures are shown. A α, β-tubulin dimer orientates with the active site (i.e., paclitaxel) of the DDMC-paclitaxel complex. The DDMC-paclitaxel complex (~270 nm) will consists of more than 8.1×10^3 DDMC molecules and 6.7×10^6 paclitaxel molecules.

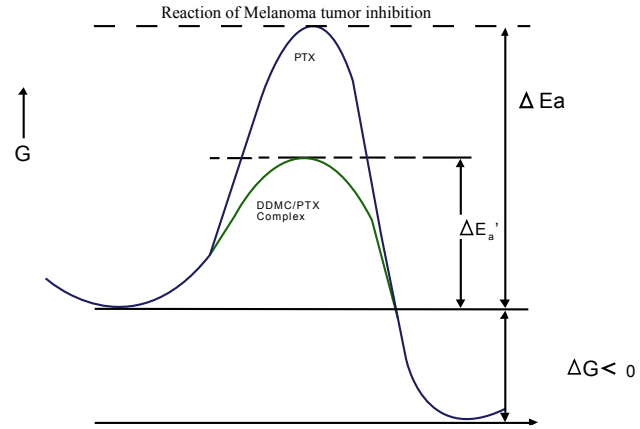

Figure 5: Potential energy curve of paclitaxel (blue) and DDMC-paclitaxel complex (green).

E_a: activation energy of paclitaxel, E_a': activation energy of DDMC-paclitaxel complex.

On the other hands, figure 5 shows small activation energy Ea′ with DDMC/ PTX complex, and the enzyme facility yields small $\Delta G^{\ddagger}$ owing to both low $\Delta S^{\ddagger}$ and low $\Delta H^{\ddagger}$, that is why apoptosis of melanoma cell(R) should be progress.

Disclosure of Potential Conflicts of Interest

No potential conflicts of interest were disclosed.

Acknowledgments

A portion of this research was carried out with the support of a Japanese Ministry of Health, Labor, and Welfare Scientific Research Grant (H23-Shinko-Ippan-015) and the Japan Society for the Promotion of Science Research Grant (Basic C 23590803).

References

1. DeVita VT (1989) Cancer: Principles and Practice of Oncology. Lippincott, Williams & Wilkins, Philadelphia.

2. Matsumura Y, Maeda H (1986) A new concept for macromolecular therapeutics in cancer chemotherapy: Mechanism of tumoritropic accumulation of proteins and the antitumor agent smancs. Cancer Res 46: 6387-6392.

3. Allen TM, Chonn A (1987) Large unilamellar liposomes with low uptake into the reticuloendothelial system. FEBS Lett 223: 42-46.

4. Oku N, Namba Y, Okada S (1992) Tumor accumulation of novel RES-avoiding liposomes. Biochim Biophys Acta 1126: 255-260.

5. Savic R, Luo L, Eisenberg A, Maysinger D (2003) Micellar nanocontainers distribute to defined cytoplasmic organelles. Science 300: 615-618.

6. Hamblin MR, Miller JL, Rizvi I, Ortel B, Maytin EV, et al. (2001) Pegylation of a chlorin(e6) polymer conjugate increases tumor targeting of photosensitizer. Cancer Res 61: 7155-7162.

7. Nishiyama N, Nori A, Malugin A, Kasuya Y, Kopecková P, et al. (2003) Free and N-(2-Hydroxypropyl) methacrylamide Copolymer-bound Geldanamycin Derivative Induce Different Stress Responses in A2780 Human Ovarian Carcinoma Cells. Cancer Res 63: 7876-7882.

8. Lehn JM (1988) Supramolecular chemistry-scope and perspectives: molecules, supermolecules and molecular devices. Angew Chem Int Ed 27: 89-112.

9. Yguerabide J, Yguerabide EE (1998) Light-scattering submicroscopic particles as highly fluorescent analogs and their use as tracer labels in clinical and biological applications. Anal Biochem 262: 137-156.

10. Nakano T, Takewaki K, Yade T, Okamoto Y (2001) Dibenzofulvene, a 1,1-diphenylethylene analogue, gives a pi-stacked polymer by anionic, free-radical, and cationic catalysts. J Am Chem Soc 123: 9182-9183.

11. Miyano S (2011) Cancer and Supercomputer. CICSJ Bulletin 29: 42-48.

12. Cheng YC, Prusoff WH (1973) Relationship between the inhibition constant (K_i) and the concentration of inhibitor which causes 50 per cent inhibition (I_{50}) of an enzymatic reaction. Biochem Pharmacol 22: 3099-3108.

13. Eshita Y, Ji RC, Onishi M, Mizuno M, Yoshida J, et al. (2012) Supramolecular Facilities to Melanoma Cells B16F10 with Nanoparticles of a DEAE-Dextran-MMA Copolymer-Paclitaxel Complex. J Nanomed Nanotechol S5: 002.

14. Hill AV (1910) The possible effects of the aggregation of the molecules of hemoglobin on its dissociation curve. J Physiol 40.

15. Xiao H, Verdier-Pinard P, Fernandez-Fuentes N, Burd B, Angeletti R, et al. (2006) Insights into the mechanism of microtubule stabilization by Taxol. Proc Natl Acad Sci USA 103: 10166-10173.